Investigation of the eta-prime meson structure and of the isospin dependence of its production in the nucleon-nucleon collisions

P. Moskal[a,b]

[a] *Institut für Kernphysik, Forschungszentrum-Jülich, Germany*

[b] *Institute of Physics, Jagellonian University, Kraków, Poland*

Abstract: It is proposed to investigate the structure of the η' meson and the mechanism of its creation in the nucleon-nucleon interaction by comparing its close to threshold production cross section in the proton-proton and proton-neutron collisions. The comparison of the ratio $R_{\eta'} = \sigma(pn \to pn\eta')/\sigma(pp \to pp\eta')$ with $R_{\eta} = \sigma(pn \to pn\eta)/\sigma(pp \to pp\eta)$ will allow to infer about the gluonium content of the η' meson and the relevance of quark-gluon degrees of freedom when considering the close to threshold production of this meson.

In the extreme case when the η' meson is created only from glue being excited in the interaction region the ratio $R_{\eta'}$ should be close to unity after the correction for the final and initial state interaction between the interacting nucleons. Whereas a production mechanism dominated by the isovector meson exchange would yield a significantly larger ratio. In the latter case it is expected to be close to a value of 6.5 as already determined for the η meson production. Together with already established excitation functions for the reactions $pp \to pp\eta'$, $pp \to pp\eta$ and partially also for $pn \to pn\eta$, the determination of the energy dependence of the total cross section for the $pn \to pn\eta'$ reaction would strengthen significantly constraints on the analysis aiming at the determination of contributions from mesonic, gluonic, nucleonic and resonance currents to the production process.

In the test measurement, using a beam of protons and a deuteron cluster target, we have proven the ability of the COSY-11 facility to study the quasi-free creation of mesons via the $pn \to pnX$ reaction. In this proposal we would like to ask for altogether 8 weeks of COSY beam-time **with an allocation of 4 weeks in the coming period** in order to determine the excitation function of the $pn \to pn\eta'$ reaction, in the excess energy range between Q = 0 MeV and Q = 30 MeV.

1 Introduction

In 1984 Maltman and Isgur [1] have argued on the basis of simple geometrical considerations (see Figure 1) that at the distances smaller than 2 fm the internucleon potential should begin to be free of meson exchange effects and may be dominated by the residual colour forces. However, the

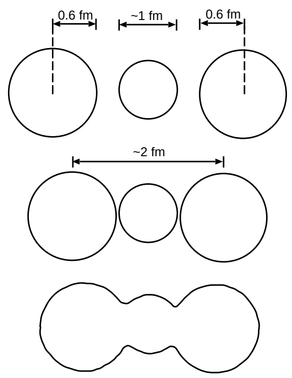

Figure 1: A cartoon illustrating in naive geometrical terms that for $r < 2r_N + 2r_M$ meson exchange is unlikely to be appropriate to the description of the internucleon potential. Figure and caption are taken from reference [1].

transition region from the hadronic to constituent quark degrees of freedom does not have a well defined boundary, and at present both approaches should be evaluated in order to test their relevance in the description of close-to-threshold meson production in the collision of nucleons. The authors of reference [2] have shown, that for example the K^+ meson production via the $pp \to pK^+\Lambda$ reaction far from its production threshold can well be described in terms of either the meson-exchange mechanism or the two-gluon exchange model. Thus, a determination of the relevant degrees of freedom for the description of the nucleon-nucleon interaction, especially in case when nucleons are very close together, remains one of the key issues in the hadronic physics [3].

Close-to-threshold production of η and η' mesons in the nucleon-nucleon interaction requires a large momentum transfer between the nucleons and hence can occur only at distances smaller than $\sim$0.3 fm. This suggests that the quark-gluon degrees of freedom may indeed play a significant role in the production dynamics of these mesons, and especially that the η' meson can be created directly from the glue which is excited in the interaction region of the colliding nucleons [4, 5]. A possibly large glue content of the η' and the dominant flavour-singlet combination of its quark wave function may cause that the dynamics of its production process in the nucleon-nucleon collisions is significantly different from that responsible for the production of the η meson (see Figure 2).

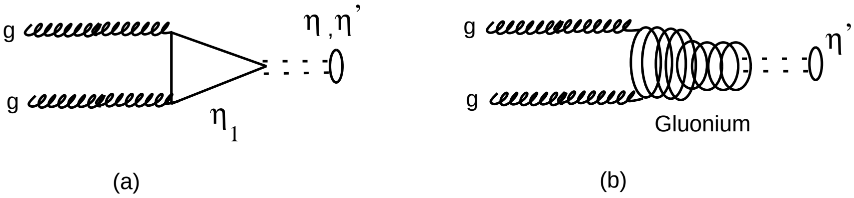

Figure 2: Coupling of η and η' to two gluons through (a) quark and antiquark triangle loop and (b) gluonic admixture.
η_1 denotes the SU(3) flavour-singlet quark-antiquark state. This indicates that gluons may convert into the η or η' meson via a triangle quark loop only by coupling through their flavour singlet part. The figure is taken from reference [6].

2 Structure of the η' meson: Does it differ from the structure of the meson η?

The η' meson was first observed in 1964 [7, 8] in the reaction $K^-p \to \Lambda\eta'$. Despite almost fourty years of investigations its structure is still not well determined. It appears that its properties cannot be described in terms of the mixture of the singlet ($\eta_1 = \frac{1}{\sqrt{3}}(u\bar{u} + d\bar{d} + s\bar{s})$) and octet ($\eta_8 = \frac{1}{\sqrt{6}}(u\bar{u} + d\bar{d} - 2s\bar{s})$) states of the SU(3)-flavour pseudoscalar meson nonet. According to this classification the amount of singlet and octet components in the physical η and η' mesons wave functions is determined by the pseudoscalar mixing angle Θ [9]:

$$\eta = cos\Theta \cdot \eta_8 - sin\Theta \cdot \eta_1, \quad \eta' = sin\Theta \cdot \eta_8 + cos\Theta \cdot \eta_1.$$

The most up to date value of this angle is determined to be $\Theta = -15.5^\circ \pm 1.3^\circ$ [10] and implies that the percentage amount of the strange and non-strange quarkonium in both mesons is almost the same:

$$\eta = 0.77 \cdot \frac{1}{\sqrt{2}}(u\bar{u} + d\bar{d}) - 0.63 \cdot s\bar{s}, \quad \eta' = 0.63 \cdot \frac{1}{\sqrt{2}}(u\bar{u} + d\bar{d}) + 0.77 \cdot s\bar{s}.$$

Thus, in this scheme, the masses of these mesons should be almost equal, but they are not. The mass of the $\eta'(958)$ meson is almost two times larger than the mass of the meson $\eta(547)$. Moreover, it is the mass of the η' meson which does not fit to the SU(3) scheme. The masses of all other members of the pseudoscalar meson nonet, including the η meson, can be described within an accuracy of 2% by a phenomenological formula which assigns the meson mass to the sum of the quark and antiquark masses and their energy of the colour spin-spin coupling [11, 12]. The difficulty in describing the η' mass becomes even more surprising when one realizes that not only the masses of pseudoscalar or vector mesons are well described in terms of quark models but also the masses of other hadrons like tensor mesons [13] or baryons [14]. However, in spite of the fact that the strange and non-strange quarkonium content of mesons η and η' is almost the same, due to the small mixing angle Θ, the η meson remains predominantly the SU(3)-flavour octet state and the η' meson the SU(3)-flavour singlet. This basic property of the η' – distinguishing it from the other pseudoscalar mesons – gives a hint for the explanation of its peculiar physical features.

In order to explain the large η' meson mass, the two-gluon annihilation process $gg \longleftrightarrow q\bar{q}$ is introduced as a contribution to the SU(3)-flavour singlet state [15, 16]. Because of the small pseudoscalar mixing angle such an additional gluon-induced interaction should mainly affect the properties of the η' which is predominantly built out of the SU(3)-flavour singlet state. To reproduce the observed η' mass, a gluonium component ranging between 29% and 53% is required [17]. A more sophisticated theoretical calculation based on the $U_A(1)$- extended chiral Lagrangian indicates that gluonic degrees of freedom generate about 300-400 MeV of both the η and η' mesons [4].

A gluonic component of the η' meson is introduced as a flavour singlet state additionally to the η_1, which couples directly to the glue [6]. Thus, the η' meson can couple to gluons not only via its η_1 singlet component and the quark and antiquark triangle loop but also directly through its gluonic admixture as shown in Figure 2. It is also possible that other states, predicted by the QCD theory, contribute to the η' wave function, as for example hybrids containig glue like $q\bar{q}g$, radially excited $q\bar{q}$ states as proposed by H. Lipkin [18], or heavier quarkonia like charmonium [19, 20, 21]. Out of the listed possibilities, the gluonium admixture is the one with the most theoretical considerations and is believed to be the most significant one [12, 13, 4, 6, 22, 23, 28, 32, 33, 34, 35]. The interest in the estimation of the gluonium content of the η' meson is also stimulated by the observation of an anomalously high η' appearance in the decays of B and D_s mesons. The branching ratio for $B^+ \to K^+\eta' = (6.5 \pm 1.7) \cdot 10^{-5}$ is much larger than the one for the corresponding η channel $B^+ \to K^+\eta < 1.4 \cdot 10^{-5}$.

Similar relations are found in the decay of the D_s meson for which $\dfrac{\Gamma(D_s^+ \to \eta'\rho^+)}{\Gamma(D_s^+ \to \eta' e^+\nu)} = 12.0 \pm 4.3$ exceeds $\dfrac{\Gamma(D_s^+ \to \eta\rho^+)}{\Gamma(D_s^+ \to \eta e^+\nu)} = 4.4 \pm 1.2$ [36, 37].

It is worth to stress that the observed branching ratios do not agree with the predictions which ignore the gluonic content of the η' [38] and also that these ratios for the η' meson differ significantly from those of the η.

The remarkable difference between the η and η' mesons is observed also in the close to threshold creation of these mesons in proton-proton collisions. The striking feature derived from experiments performed at CELSIUS [39, 40], SATURNE [41, 42, 43, 67], and COSY [44, 68, 69] is that the total cross sections for the $pp \to pp\eta'$ reaction is by about a factor of fourty smaller than the cross sections for the $pp \to pp\eta$ reaction at corresponding values of the excess energy. Trying to explain this large difference Hibou et al. [43] showed that a one-pion-exchange model with the parameters adjusted to fit the total cross section for the $pp \to pp\eta$ reaction underestimates the η' data by about a factor of two. This discrepancy suggests that short-range production mechanisms as for example heavy meson exchange, mesonic currents [61], or more exotic processes like the production via a fusion of gluons [28] may contribute significantly to the creation of η and η' mesons [45].
The momentum transfer required to create these mesons is much larger compared to the pion production, and already in case of pions a significant contribution from the short-range heavy meson exchange is necessary in order to obtain agreement with the experiments [46, 47]. S. Bass et al. pointed out that the axial anomaly gluonic degrees of freedom may affect the threshold behaviour of η and η' photo- and proton-induced production inducing new gluonic coupling constants in the η and η' nucleon interactions [4].
At present, since the effective coupling constant describing the η'-proton-proton vertex is not known, it is even not possible to determine the contribution from the simplest possible production mechanism where the η' is supposed to be emitted as a bremsstrahlung radiation from one of the colliding protons as shown in Figure 4a. **Consequently, investigations of the η' production have to deal with a few problems at the same time. Namely: unknown reaction mechanism, unknown coupling**

constant, and unknown proton-η' interaction.[1]

The main difficulty in the determination of the $g_{NN\eta'}$ coupling constant is due to the fact that usually the direct production on the nucleon is either associated with the production through baryonic resonances, as in the case of the $\gamma p \to \eta' p$ reaction [64, 48, 49], or with the exchange of other mesons. Therefore, if the direct production mechanism is not dominant it is not possible to extract the $NN\eta'$ coupling without the clear understanding of the other mechanisms. However, it would be very interesting to determine the $g_{NN\eta'}$ coupling constant and to compare it with calculations performed on the quark level assuming the η' meson structure.

A first theoretical attempt to determine this quantity on the quark level shows that due to the 't Hooft interaction [50] the η'-quark coupling $g_{q\bar{q}\eta'}$ is significantly suppressed compared to the other pseudoscalar mesons. Consequently, the $\eta' NN$ vertex appears to be suppressed as compared to the ηNN one [51]. The anomalous coupling of the η'-gluon-gluon vertex is also widely discussed in context of the unexpectedly large B meson decays into η' and strange mesons [34, 52, 32], but also in view of the threshold η' production

The proton-η' interaction is at present studied by the COSY-11 collaboration. In the 7'th of October 2003 we have finished the measurement of the $pp \to pp\eta'$ reaction at excess energy of Q=15.5 MeV. The missing mass spectrum determined on-line from the 10% of the data written on tapes is shown in figure 3. We estimate that the overall number of registered $pp \to pp\eta'$ events amounts to 15000. The data analysis aiming in the determination of the Dalitz plot distribution is in progress.

1

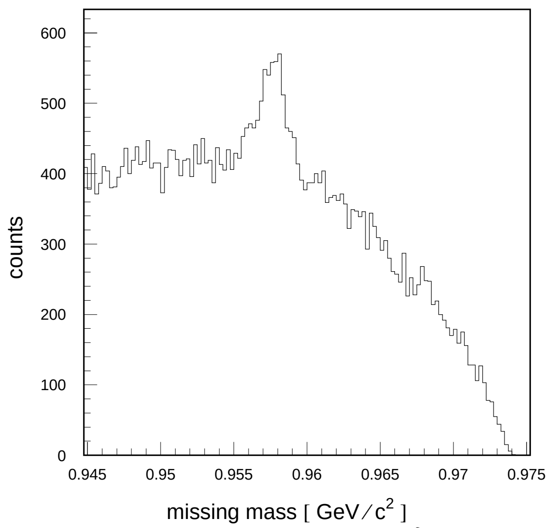

Figure 3: On-line missing-mass distribution of the $pp \to ppX$ reaction measured by means of the COSY-11 detection system in October 2003.

in the $pp \to pp\eta'$ reaction [28]. The present estimations for $g_{NN\eta'}$ deduced from different experiments are widely spread from 0.2 to 7.3 and are not consistent with each other [53]. More efforts are needed on the experimental as well as on the theoretical side to fix this important parameter.
The second interesting observation from the close to threshold production of η and η' is that the energy dependence of the total cross section for the reaction $pp \to pp\eta$ does not follow the predictions based on the phase space volume and the proton-proton final state interaction, which, however, is the case for the η' meson production in the $pp \to pp\eta'$ reaction.

The primary production amplitude for η' normalized to the one for the π^0 was found to be independent of the excess energy. In contrary, in case of η this normalized amplitude increases with decreasing energy [70]. Thus it was concluded that the η' meson interacts with the proton much weaker than the η [70], albeit both these mesons have very similar quark contents. Again, the gluonic admixture of η' will influence the η'-nucleon interaction via the U(1) anomaly [28]. The range of the glue induced η'-nucleon interaction, if determined by the two-gluon effective potential, would be in the order of 0.2-0.4 fm [54]. This is already large enough to be important in the threshold production of η' via the reaction $NN \to NN\eta'$ which occurs when the colliding protons are closer than 0.2 fm.

What is the mechanism of η' production in the $NN \to NN\eta'$ reaction ?

Theoretical studies of the production mechanisms accounting for the π^0 and η mesons creation in the close to threshold $pp \to pp\pi^0(\eta)$ reactions have shown that the short-range component of the N-N force and the off-shell pion rescattering dominate the production process of the π^0 meson [46, 47, 55], whereas the η meson is predominantly produced through the excitation of the intermediate baryonic resonance $S_{11}(1535)$[56, 57, 58, 59, 39]. However, the comparison of the experimentally determined η and η' ratio of the total cross sections with the predictions based on the one-pion-exchange model indicates that we are still far from the full understanding of the dynamics of the discussed processes. In particular, at present there is not much known about the relative contribution of the possible reaction mechanisms to the production of the η' meson. It is expected that – similarly to the case of pions – the η' meson can be produced as depicted in Figures 4a,b,c,d. However, because of the much larger four-momentum transfer short-range mechanisms – like heavy meson exchange (Figure 4c) or production via a mesonic current

(Figure 4e), where the η' is created in a fusion of exchanged virtual ω, ρ, or σ mesons – are expected to contribute even more significantly.

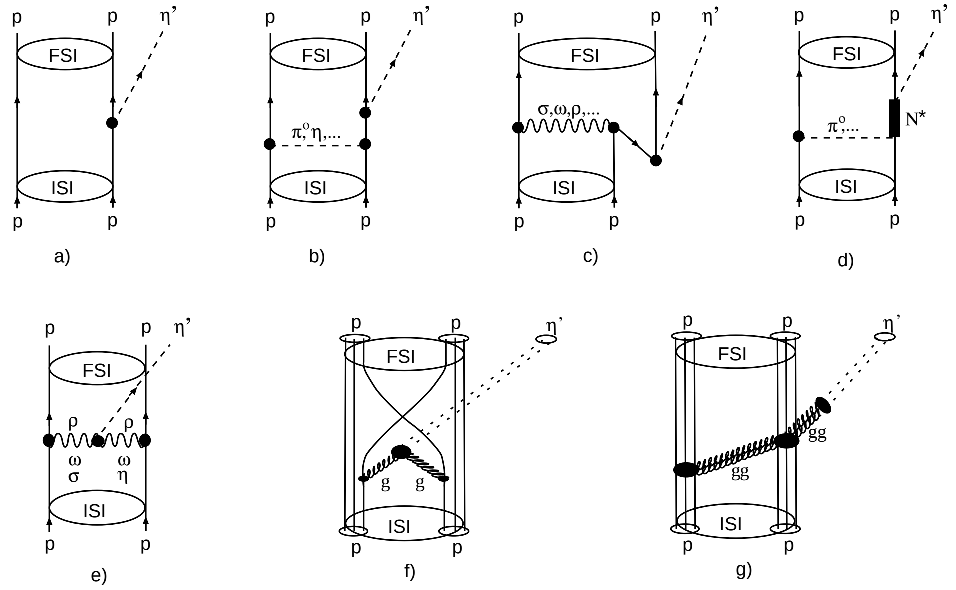

Figure 4: Diagrams for the $pp \to pp\eta'$ reaction near-threshold: (a)— η'-bremsstrahlung (nucleonic current) (b)— "rescattering" term (nucleonic current) (c)— production through heavy meson exchange (d)— excitation of an intermediate resonance (nucleon resonance current) (e)— emission from the virtual meson (mesonic current)
(f),(g) Diagrams depicting possible quark-gluon dynamics of the reaction $pp \to pp\eta'$
(f)— production via a fusion of gluons [5] with rearangement of quarks (gluonic current). (g)— production via a rescattering of a "low energy pomeron" [60] (gluonic current).

The understanding of the η' production on the hadronic level is far from being satisfactory. Recently, Nakayama et al. [61], studied contributions from the *nucleonic* (Fig. 4b), *nucleon resonance* (Fig. 4d), and *mesonic* (Fig. 4e) currents and found that each one separately could describe the absolute values and energy dependence of the close to threshold η' data points [43, 69], after an appropriate adjustment of the ratio of the pseudoscalar to the pseudovector coupling. Among the mesonic currents regarded by authors of reference [61] the $\rho\rho\eta'$ gives the dominant contribution, by a factor of five larger than the $\sigma\eta\eta'$– and $\omega\omega\eta'$–exchange. The magnitude of the total cross section was also well reproduced in the frame of a one–boson–exchange model (nucleonic current) where the virtual boson ($B = \pi, \eta, \sigma, \rho, \omega, a_0$) created on one of the colliding protons converts to the η' on the other one [62]. Taking into account the off–shell effects of the $Bp \to \eta' p$ amplitude it was found that the short range σ and ρ meson exchanges dominate the creation process, whereas the π exchange plays a minor role. On the contrary, other authors [63] reproduced the magnitude of the total cross section with π exchange only and concluded that the η, ρ and ω exchange currents either play no role or cancel each other. However, in both of the above quoted calculations [62, 63] the initial state interaction between protons, which reduces the rate by a factor of about 3, was not taken into account and hence the obtained results would in any case reproduce only 30 % of the entire magnitude and could be at least qualitatively reconciled with the mentioned result of reference [61], where the nucleonic current was found to be small. Moreover, the choice of the another prescription for the form factors could reduce the one–pion–exchange contribution substantially [61]. However, the picture that the η' meson is predominantly created through the mesonic current, remains at present unclear as well. This is because the magnitude of the total cross section could have been also described assuming that the production of η' is resonant [61]. As possible intermediary resonances the recently reported [64] $S_{11}(1897)$ and $P_{11}(1986)$ have been considered. These resonances were deduced from η' photoproduction data, under the assumption that the close–to–threshold enhancement observed for the $\gamma p \to \eta' p$ reaction can be utterly assigned to resonance production. Further, as well strong, assumptions have been made in the derivation of the $g_{NN^*\eta'}$ and $g_{NN^*\pi}$ coupling constants [61].

The above discussion shows that **it is not possible to judge about the mechanisms responsible for the η' meson production from the total cross section of the reaction $pp \to pp\eta'$ only. This rather pessimistic conclusion calls for further experimental and theoretical research.**

The understanding of the production dynamics of the η' meson on both hadronic and the quark–gluon level is particularly important since its wave function comprises a significant gluonic component [33], distinguishing it from other mesons and hence the comprehension of the mechanism leading to its creation in collisions of hadrons may help in the determination of its quark–gluon structure which is also of importance to investigate possible glueball candidates [33]. Hereafter we will briefly report about the gluonic mechanisms which may — additionally to the meson exchange processes discussed above — contribute to the η' production. As already mentioned, the close–to–threshold production of η and η' mesons in the nucleon–nucleon interaction requires a large momentum transfer between the nucleons and hence can occur only at distances of about 0.3 fm. This suggests that the quark–gluon degrees of freedom may indeed play a significant role in the production dynamics of these mesons. A possibly large glue content of the η' and the dominant flavour–singlet combination of its quark wave function may cause that the dynamics of its production process in nucleon–nucleon collisions is significantly different from that responsible for the production of other mesons. In particular, the η' meson can be efficiently created via a "contact interaction" from the glue which is excited in the interaction region of the colliding nucleons [28]. A gluon–induced contact interaction contributing to the close–to–threshold $pp \to pp\eta'$ reaction derived in the frame of the U(1)–anomaly extended chiral Lagrangian is discussed in references [28, 4, 29]. The strength of this contact term is related to the amount of spin carried by polarized gluons in a polarized proton [29, 30], thus making the study of the close–to–threshold η' meson production even more interesting. **The created gluons could couple to the η' meson directly via its gluonic component or through its flavour-singlet admixture η_1 (see Figure 2).**

Figures 4f and 4g depict possible short-range mechanisms which may lead to the creation of the flavour singlet state via a fusion of gluons emitted from the exchanged quarks of the colliding protons [5] or via an exchange of a colour-singlet object made up from the glue, which then rescatters and converts into η'[60]. In contrary to the meson exchange mechanisms and the fusion of gluons of graph f, the production through the colour-singlet object proposed by Steven D. Bass (graph g) is isospin independent, and hence should lead to the same production yield of the η' meson in the $pp \to pp\eta'$ and $pn \to pn\eta'$ reactions after correcting for the final and initial state interaction between the nucleons.

In case of the η meson both these reaction channels were already measured. The ratio $R_\eta = \dfrac{\sigma(pn \to pn\eta)}{\sigma(pp \to pp\eta)}$ was determined to be about 6.5 in the excess energy range between 16 MeV and 109 MeV [72]. This implies that the production of the η meson with the total isospin equal to zero exceeds the production with the isospin $I = 1$ by a factor of 12, since $\sigma(pn \to pn\eta) = \dfrac{\sigma_{I=0} + \sigma_{I=1}}{2}$, and $\sigma(pp \to pp\eta) = \sigma_{I=1}$, and hence $\sigma_{I=0} = (2R_\eta - 1)\sigma_{I=1}$. This large difference of the total cross section between the isospin channels suggests the dominance of isovector meson (π and ρ) exchange in the creation of η in nucleon-nucleon collisions [45, 72].

The comparison of the $pn \to pn\eta'$ and $pp \to pp\eta'$ total cross sections will allow to compare the production of the η' meson in the channels of isospin I = 0 and I = 1. By analogy to η production, in case of a dominant isovector meson exchange mechanism the ratio $R_{\eta'}$ is expected to be about 6.5. In the other scenario, when the η' is produced via its flavour-singlet or gluonic component from the colour-singlet glue excited in the interaction region, the ratio $R_{\eta'}$ should approach unity after the correction for the final and initial state interactions between the participating baryons [31]. This is because the glue does not distinguish between flavours.

Figures 5 and 6 demonstrate qualitatively the fact that the production of mesons in the proton-neutron collisions is more probable than in the proton-proton one if only the production is driven by the isovector meson exchanges. This is because in the case of the proton-neutron collisions there are always more possibilities to realise the exchange or fusion of the isovector mesons than in the case of the reaction of protons.

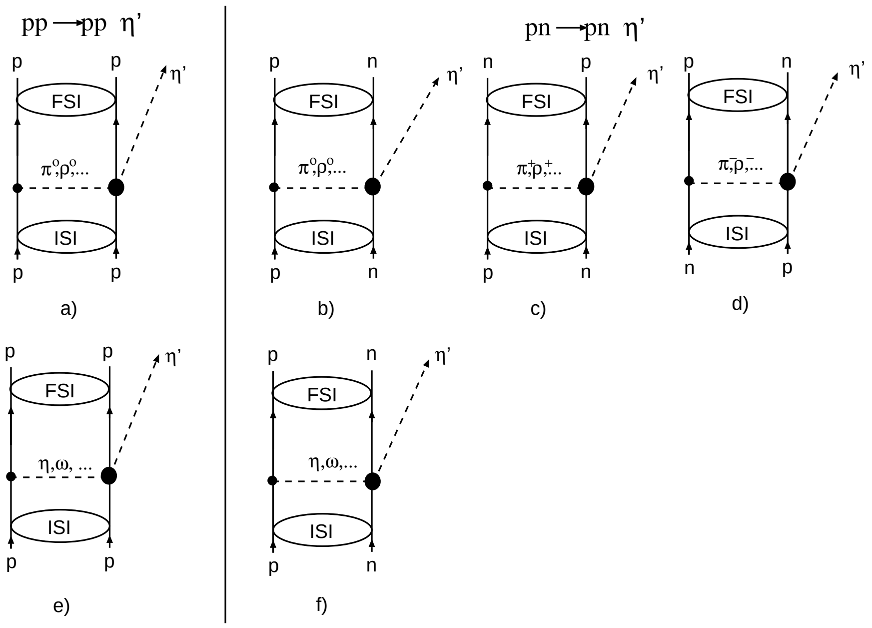

Figure 5: Example of diagrams with the isovector and isoscalar meson exchange leading to the creation of the meson η' in the proton-proton and proton-neutron collisions.

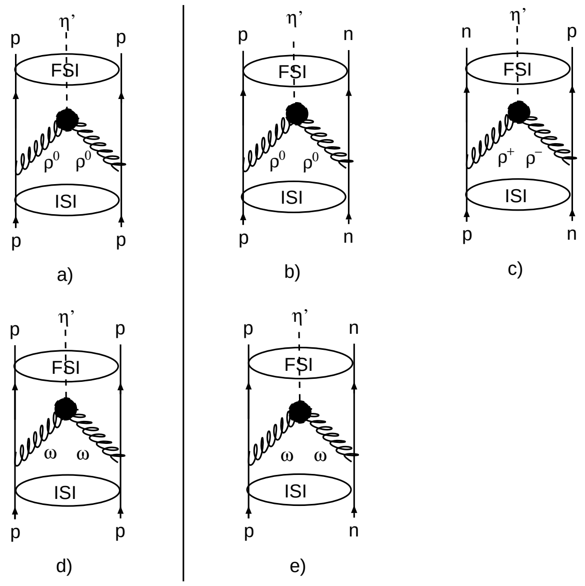

Figure 6: Fusion of the virtual ω and ρ mesons emitted from the colliding nucleons.

In addition to the QCD motivated investigation presented above [28, 4], the interesting features of the close–to–threshold meson production, in particular the large cross section for the η meson in proton–proton interactions exceeding the one of the pion, or even more surprisingly large cross section of the η production in proton–neutron collisions, encouraged also other authors to seek for the underlying — OZI rule violating — creation mechanisms in the frame of microscopic models of QCD [25, 26, 2]. The hitherto regarded processes are presented in figure 7. As indicated in the pictures the structure of participating baryons has been modeled as quark–diquark objects with harmonic confinement [27]. In the upper graphs the large momentum transfer is shared by the exchanged gluons with a subsequent interchange of quarks to provide a colourless object in the final state. The lower graphs depict the two examples of instanton induced interactions with a 6–quark–antiquark (fig. 7d) and two-gluon vertex (fig. 7e).

Adjusting the normalization to the cross section of the $pp \to pp\pi^0$ reaction at a single energy point the model [26] accounts roughly for close–to–threshold cross sections of other pseudoscalar and vector mesons in proton–proton collisions. Though this approach is characterized by significantly smaller number of parameters than in the meson exchange models, their uncertainties allow for the description of the data equally well either by the gluon exchange or by the instanton induced interactions, at least in case of the π^0, η', ω and ϕ mesons. Yet for the resonance dominated η and K^+ meson production in proton–proton collisions it was found that the instanton induced interaction presented by graph 7d is not sufficient. Similarly, the authors of reference [25] argue that the instanton induced interaction with a quark–gluon vertex (graph 7e) should be of no importance for the η production in proton–proton collisions. This arises from the properties of the vertex which lead to the η production only in case of an interaction between quarks of different flavours ($ud \to udgg$) and in the quark–diquark model of baryons the proton consists of ud–diquark and u–quark and correspondingly the neutron is modeled as ud–diquark and d–quark. Although negligible in case of proton–proton interactions, this mechanism may contribute significantly to the total cross section of the $pn \to pn\eta$ reaction and indeed as shown in reference [25] it reproduces the data.

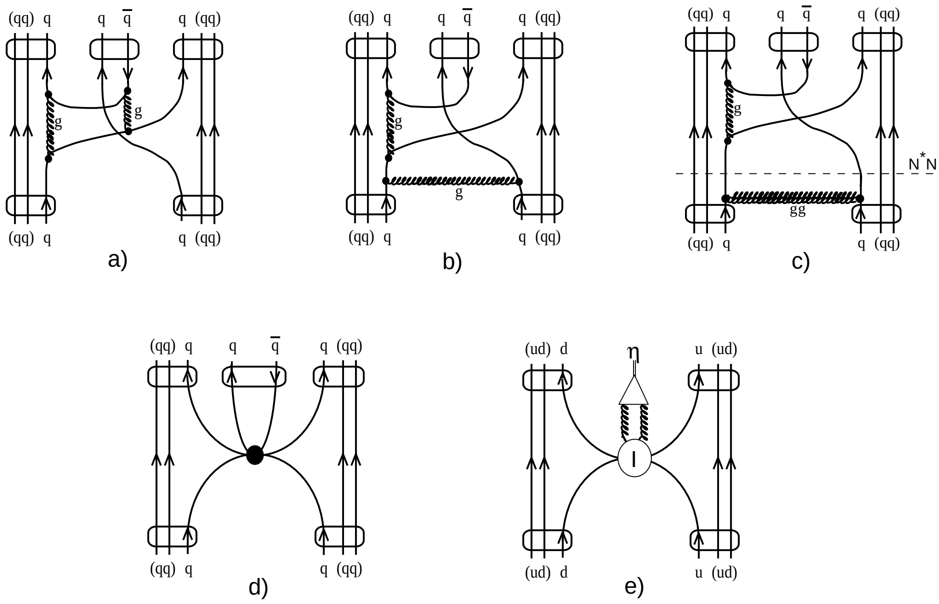

Figure 7: Diagrams for the $qq \to qq(q\bar{q})$ production operator: (a), (b) Two–gluon exchange and rescattering mechanism (c) Correlated, colourless two-gluon exchange. The dashed line indicates the excitation of an intermediate NN^* system. (d) Instanton induced 6–quark interaction. Figures (a–d) according to [26]. (e) The instanton contribution to the η meson production in the proton–neutron interaction. Figure copied from [25].

However, the magnitude of the cross section is very sensitive to the size of the instanton in the QCD vacuum and — similar to the uncertainty of coupling constants in case of the hadronic approach — at present it makes precise predictions impossible. Thus, despite the partial successes, at the present stage of developments both approaches — on the quark–gluon and on the hadronic level — do not deliver an unambiguous answer to the dynamics of the close–to–threshold meson production in the nucleon–nucleon interaction.

3 Method of measurement: Simulations of the quasi-free $pn \to pn\eta'$ reaction

In order to measure the $pn \to pn\eta'$ reaction by means of a proton beam it is necessary to use a nuclear target, since a pure neutron target does not exist. Similar to investigations of the η meson production in the $pn \to pn\eta$ reaction [73, 40, 72], a deuteron will be considered as source of neutrons. Due to the small binding energy of the deuteron ($E_B = 2.2$ MeV), the neutron struck by the proton incoming with 2540 MeV kinetic energy may approximately be treated as being a free particle in the sense that the matrix element for quasi-free meson production on a bound neutron is identical to that for the free $pn \to pn\eta$ reaction. Measurements performed at CELSIUS [40, 72] and TRIUMF [65, 66] have proven that the offshellness of the reacting neutron can be neglected and that the spectator proton influences the interaction only in terms of the associated Fermi motion [65]. In this approximation the proton from the deuteron is considered as a spectator which does not interact with the bombarding proton, but rather escapes untouched and hits the detectors carrying the Fermi momentum possessed at the moment of the collision. The momentum spectrum of the nucleons in the deuteron is shown in Figure 8a. Since the neutron bound inside a deuteron is not at rest, and its momentum may change from event to event, the excess energy in the quasi-free proton-neutron reaction will also vary from event to event. This enables to scan a large range of excess energies with a constant proton beam momentum, but simultaneously requires the determination of this energy for each registered event, which can be done only if the neutron momentum vector is known. This may be realized experimentally either by determining the four-momentum vectors of the outgoing proton, neutron, and η' or by measuring the four-momentum of the spectator proton. The latter possibility is realised at the COSY-11 facility.

From the measurement of the momentum vector of the spectator proton one can infer the momentum vector of the neutron at the time of the reaction, and hence calculate the excess energy. The distribution of the excess

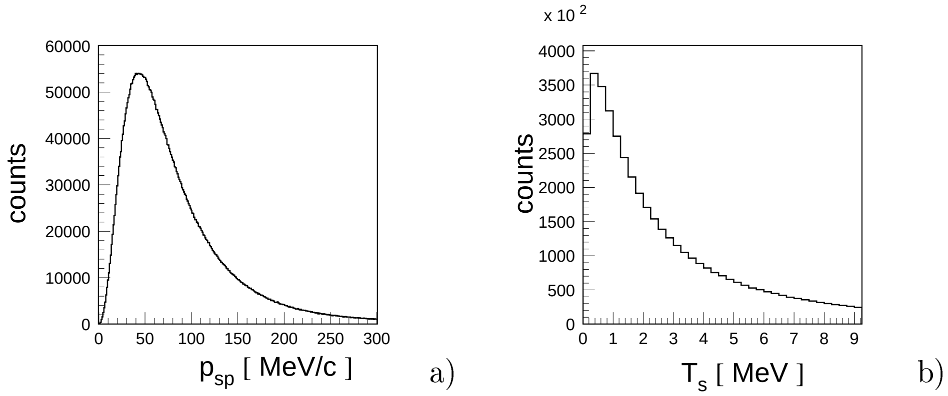

Figure 8: (a) Momentum and (b) kinetic energy distribution of the nucleons in the deuteron, generated according to an analytical parametrization of the deuteron wave function [74, 75] calculated from the PARIS potential [76].

energy in a quasi-free $pn \to pn\eta'$ reaction is presented in Figure 9a. In the framework of the so-called impulse approximation the spectator proton is a physical particle, hence it must be on its mass shell. This implies, however, that the reacting neutron is off its mass shell, and hence the extrapolation from the quasi-free to the free $pn \to pn\eta'$ must be done with care. The distribution of the off-shell mass of the interacting neutron is shown in Figure 9b. It can be seen that the maximum of this spectrum differs only by about 3 MeV from the free neutron mass ($m_n = 939.57$ MeV), however on the average it is off by about 9 MeV. Measurements performed at the CELSIUS and TRIUMF accelerators for the $pp \to pp\eta$ [40] and $pp \to d\pi^+$ [65] reactions, respectively, have shown that within the statistical errors there is no difference between the total cross section of the free and quasi-free processes (see figure 10). The quasi-free production were realized utilizing a deuteron target. This observation allows to anticipate that in the case of the planned study of the η' in the $pd \to p_{sp}np\eta'$ reaction, the measured total cross section for the quasi-free $pn \to pn\eta'$ reaction will not differ from the on-shell one. In fact, the difference between off-shell and on-shell cross section of the η' meson production should be even smaller than in the case of the η and π, since in the former case the total energy of the interacting nucleons is much larger than in the latter one, and the mean difference between the off-shell and on-shell neutron mass remains the same.

Other nuclear effects in case of the production on the neutron bound in the nucleus are rather of minor importance. The effect of the reduction of the beam flux on a neutron due to the presence of the proton in the deuteron,

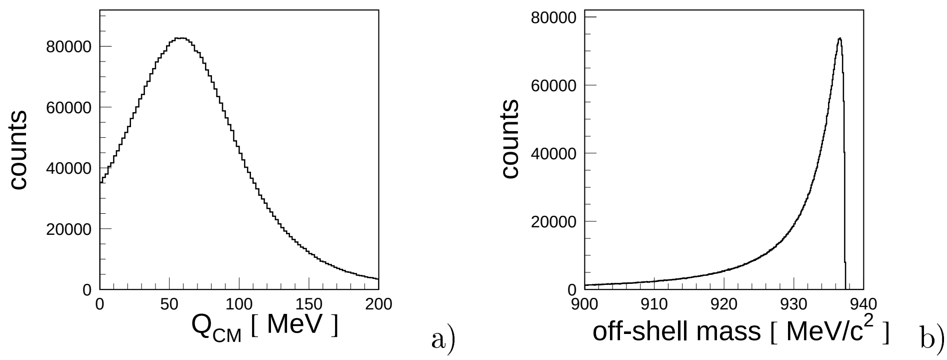

Figure 9: (a) Distribution of the excess energy Q_{CM} for the $pn\eta'$ system originating from the reaction $pd \to p_{sp}pn\eta'$ calculated with a proton beam momentum of 3.350 GeV/c, and the neutron momentum smeared out according to the Fermi distribution shown in Figure 8b. The beam momentum of 3.350 GeV/c corresponds to an excess energy of $Q_{CM} = 44.7$ MeV for the free $pn \to pn\eta'$ reaction.
(b) Spectrum of the off-shell mass of the interacting neutron, as calculated under the assumption of the impulse approximation.

referred to as a shadow effect, decreases the total cross section by about 4.5% in case of η production [73]. Thus it should also have a minor influence on the evaluation of the total cross section for the $pn \to pn\eta'$ reaction. Similarly the reduction of the total cross section due to the reabsorbtion of the produced η' on the spectator proton should be negligible due to the weak [70] proton-η' interaction. Even in case of the η meson, which interacts with protons much more strongly, this effect was found to be only about 3% [73].

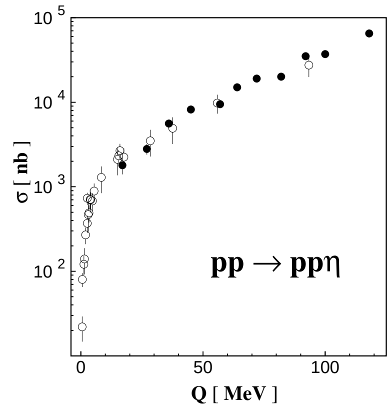

Figure 10: (a) Total cross sections for the $pp \to pp\eta$ reaction as a function of excess energy measured for the scattering of protons in vacuum (open symbols) [44, 43, 39, 42, 41, 53] and inside a deuteron (filled symbols) [40].

In order to identify the production of the η' meson in a proton-deuteron collision it is necessary either to measure the decay products of the meson or to register the outgoing nucleons and nuclei.

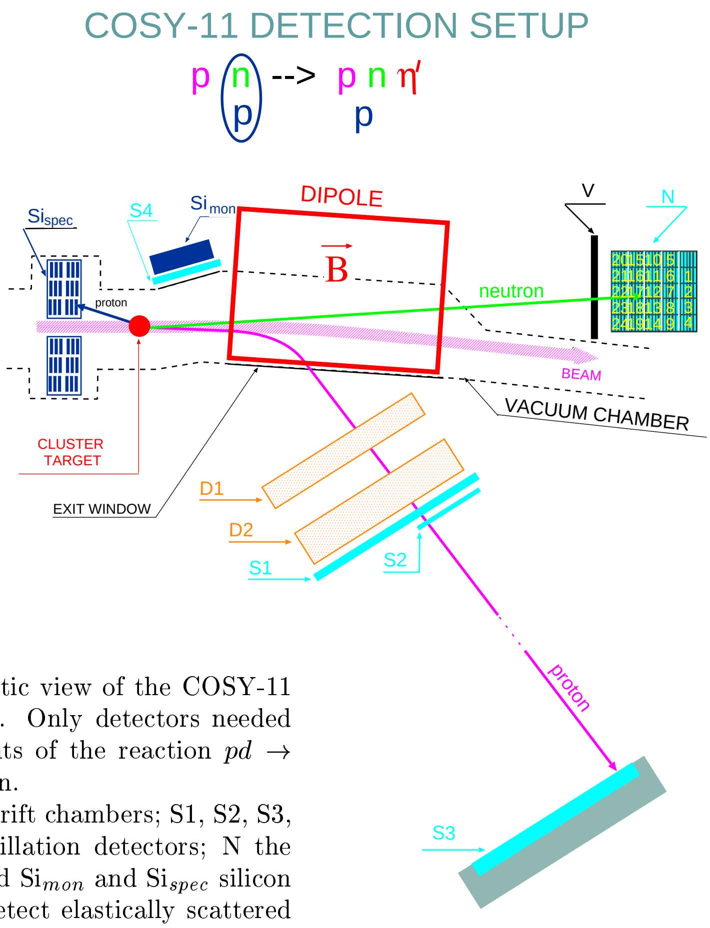

Figure 11: Schematic view of the COSY-11 detection setup [77]. Only detectors needed for the measurements of the reaction $pd \rightarrow p_{sp}pn\eta(\eta')$ are shown.
D1, D2 denote the drift chambers; S1, S2, S3, S4 and V the scintillation detectors; N the neutron detector and Si_{mon} and Si_{spec} silicon strip detectors to detect elastically scattered and spectator protons, respectively.

The proposed investigation is planned to be performed using the COSY-11 detection system with an additional silicon strip detector for the registration of the spectator proton.

In Figure 11 a schematic view of the COSY-11 detection system together with the spectator detector is presented. The spectator detector [71] consists of four modules with two layers of 0.3 mm thick silicon strips. Each module is further divided into six parts each of them with 3 strips of 20 mm x 5 mm. The physical properties of the detector were implemented into the COSY-11 Monte-Carlo programme and detailed simulations of the $pd \rightarrow p_{sp}pn\eta'$ reaction were performed, taking into account the momentum and dimension spread of the COSY beam [78], as well as the dimensions of the cluster target [79] and the known resolution of the time and position measurements of the standard COSY-11 detectors.

Figure 12a depicts the spectrum of the spectator proton momentum which will be registered in coincidence with the forward flying proton and neutron. A 300 μm thick silicon detector can absorb protons up to a momen-

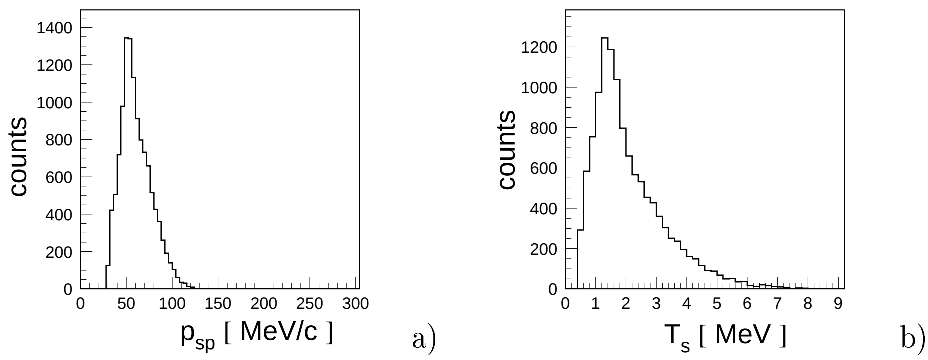

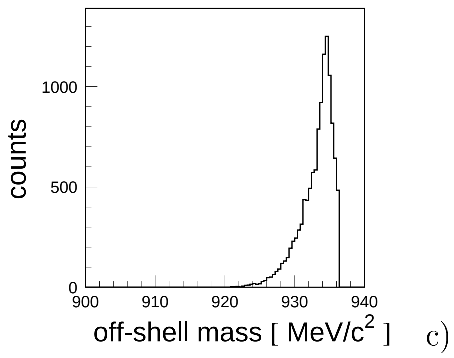

Figure 12: (a) Momentum and (b) kinetic energy distributions of the spectator protons registered in coincidence with the forward scattered neutron and proton. (c) Spectrum of the off-shell mass of the interacting neutron, provided that all nucleons from the $pd \rightarrow p_{sp}pn\eta'$ reaction have been measured with the COSY-11 detection system.

tum of about 106 MeV/c corresponding to a kinetic energy of $T_s \approx 6$ MeV. Both layers together can absorb protons up to a momentum of 130 MeV/c ($T_s \approx 9$ MeV), however, protons with momenta lower than 30 MeV/c ($T_s \approx 0.5$ MeV) cannot be distinguished from noise. Thus this detector allows the registration and identification of about 70% of the spectator protons hitting its sensitive area (see Figure 8). On the other hand, Figure 12b shows that the fraction of spectator protons having kinetic energy larger than 6 MeV and registered simultaneously with the forward scattered neutron and proton is very small. Consequently, most of the spectator protons will be fully stopped already in the first layer. This gives the opportunity to get rid of the background due to fast protons and pions crossing both layers of the detector, just by considering in the off-line analysis only those events which have no signal in the second layer.

Both the position of the spectator detector and the proton beam momentum were optimized such that most of the registered events have an excess energy between 0 MeV and 25 MeV. This is the range for which the total cross section of the $pp \to pp\eta'$ has been studied at COSY-11 [68]. Increasing the beam momentum in general shifts the maximum of the excess energy distribution (fig. 9a) to larger values, but simultaneously installing the spectator detector upstream the target (see Figure 11), such that the spectator proton is moving opposite to the proton beam, the excess energy is decreasing, since the neutron is escaping the beam proton. Positioning of the tagger detector upstream the target also reduces drastically its irradiation. The distribution of the excess energy for events registered under the chosen geometry is shown in Figure 13a. In the first approximation it reflects the dependence of the COSY-11 acceptance on the excess energy. Figure 13b depicts the difference between the generated and reconstructed excess energy. The standard deviation of the obtained resolution amounts to 2 MeV, and is due to the finite dimension of the beam and target and the granularity of the spectator detector. In these simulations the distance between the beam and the detector was adjusted to be 5 cm as an optimum regarding both the coverage of the solid angle and the angular resolution. Apart from the excess energy, in order to identify the reaction it is necessary to determine the momentum vectors of the registered protons and neutrons. Proton momenta will be reconstructed by tracking back the proton trajectory to the target point, and the neutron momenta will be determined from the time of flight between the target and neutron detector and the angle defined by the middle of the hit segment. The granularity of the neutron detector allows to determine the horizontal position with an accuracy of ± 4.5 cm. For the time resolution of one segment (11 scintillation and 11 lead plates) a conservative value of 0.5 ns (standard deviation) was assumed. The missing mass spectrum, reconstructed from events for which signals from the spectator detector as well as the forward scattered protons and neutrons were registered, is shown in Figure 14. An obtained mass resolution amouts to 7.6 MeV (FWHM) which is only 3 times the resolution of the measurements for the $pp \to pp\eta'$ reaction at an excess energy of 23.6 MeV.

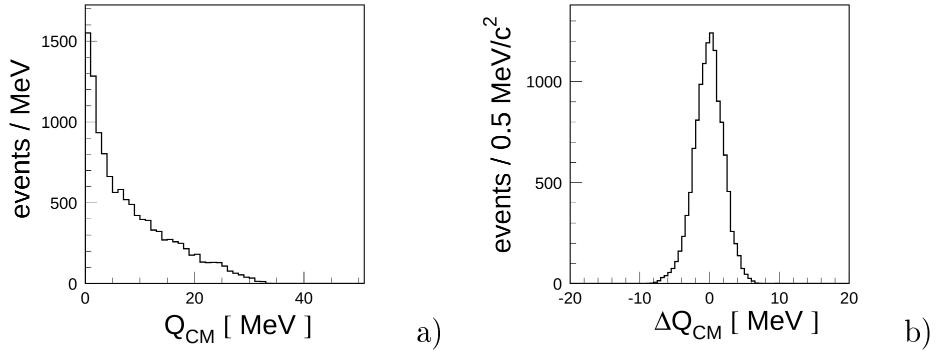

Figure 13: (a) Distributions of the excess energy Q_{CM} for the quasi-free $pn \to pn\eta'$ reaction as would be measured with the COSY-11 detection system at a beam momentum of 3.350 GeV/c. The shape corresponds roughly to the energy dependence of the detection efficiency. The Figure shows the number of reconstructed events per 1 MeV bin out of the $5 \cdot 10^6$ events generated in the target. (b) Difference between the generated and reconstructed excess energy. Calculations were performed assuming a target diameter of 0.9 cm [79], and standard deviations of 0.2 cm and 0.4 cm for the horizontal and vertical beam spread, respectively. The applied values correspond to a realistic estimation of the beam parameters based on the data from previous COSY-11 experiments [78]. The spectator detector modules were positioned behind the target, five centimeters from the beam, as it is indicated in Figure 11.

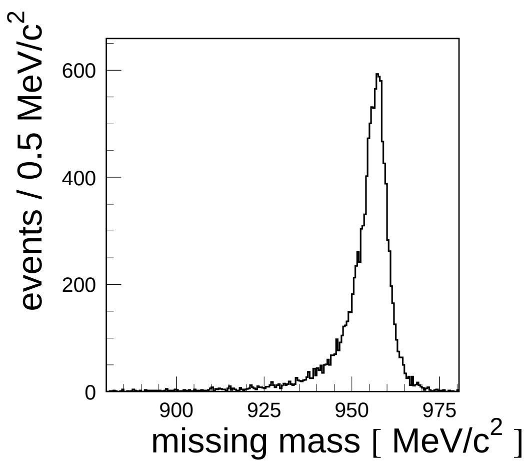

Figure 14: The missing mass distribution with respect to the pn subsystem from the reaction $pn \to pn\eta'$ as reconstructed from the generated events under the described assumptions of the time and position resolution of the COSY-11 detectors.

4 Test measurement of the $pn \to pn\eta$ reaction

As a first step towards a study of the $pn \to pn\eta'$ reaction, and as a general commissioning of the extended COSY-11 facility to investigate quasi-free $pn \to pnX$ reactions, we have performed a measurement of the $pn \to pn\eta$ reaction at a beam momentum of 2.075 GeV/c. The experiment, carried out in June 2002, had been preceded by the installation of a spectator and a neutron detectors, and by a series of thorough simulations performed in order to determine the best conditions for measuring quasi-free $pn \to pn\eta$ and $pn \to pn\eta'$ reactions. Results of the test are compared to the Monte-Carlo simulations in the following figures. Though at present only a rough calibration of the neutron and spectator detector have been performed one recognizes a well agreement between the expectations and the experimental results.

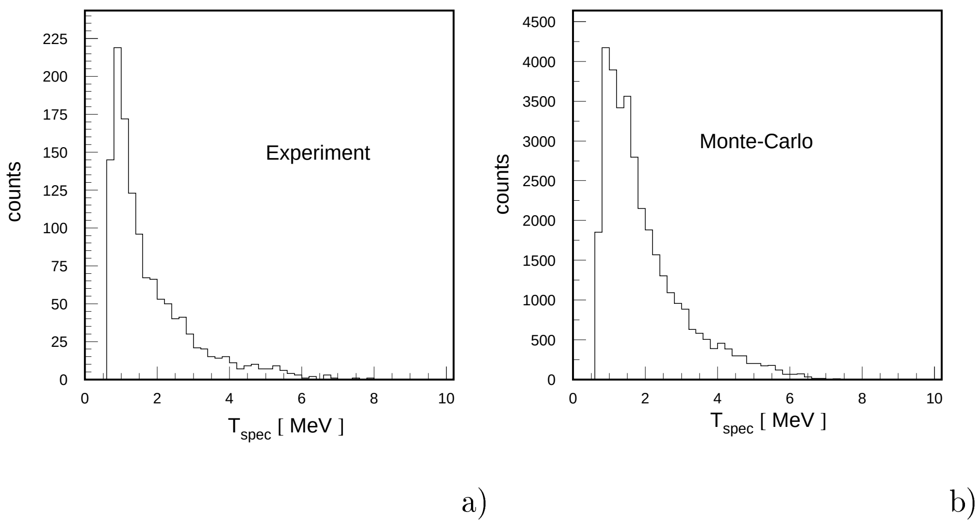

Figure 15: Distributions of the kinetic energy of the spectator protons.
(a) Experiment.
(b) Monte-Carlo Simulations.

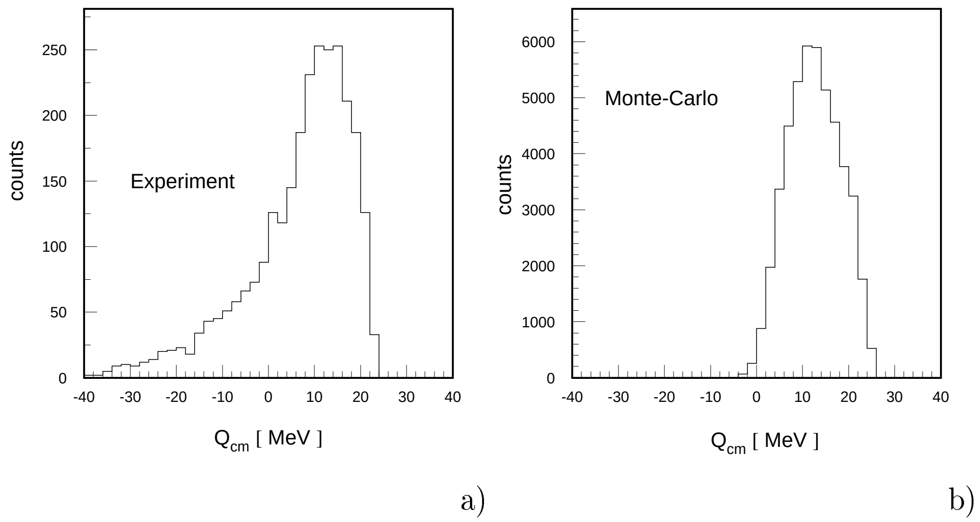

Figure 16: (a) Distributions of the excess energy Q_{CM} for the quasi-free $pn \to pnX$ reaction, calculated with respect to the $pn\eta$ threshold.

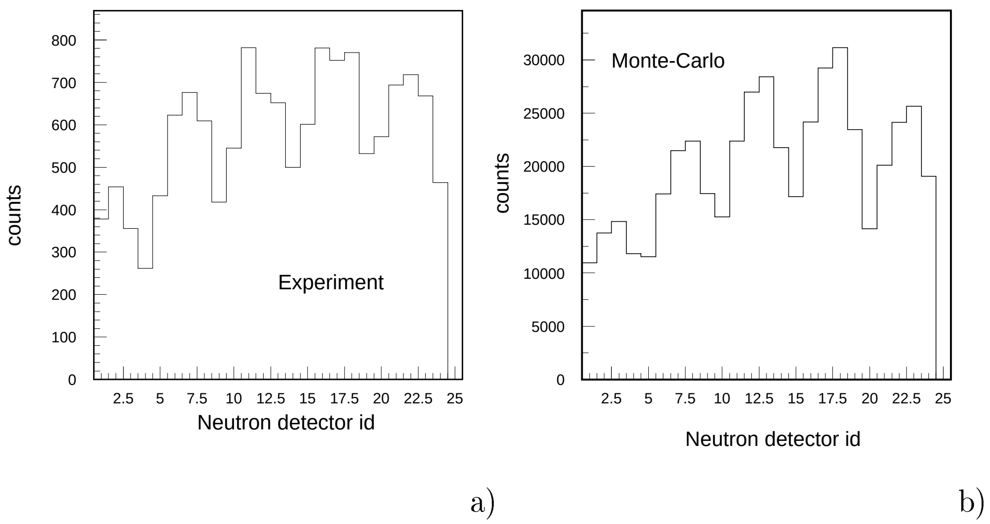

Figure 17: Number of hits per individual module of the neutron detector. Module id's are defined in figure 11.
a) As obtained in the experiment. b) Monte-Carlo simulation.

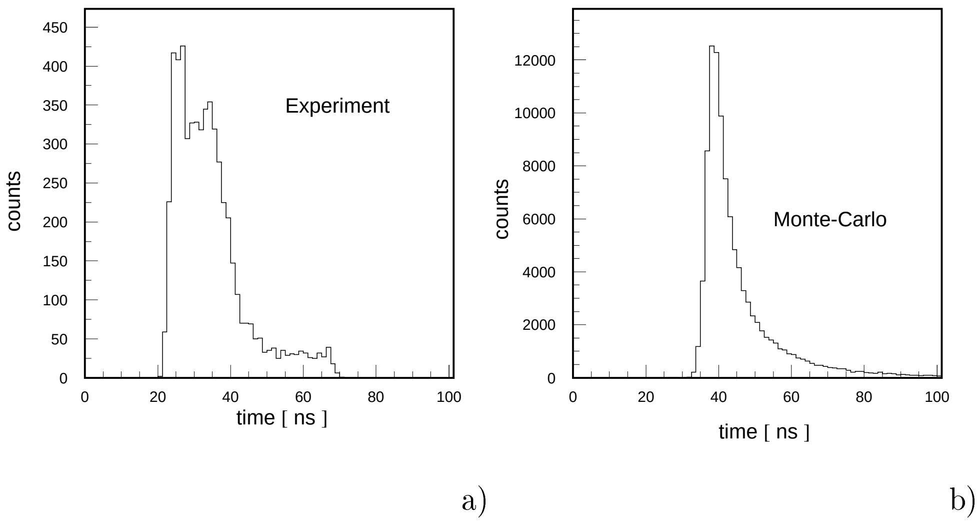

Figure 18: Time of flight distribution determined between the target and the neutron detector. Simulation corresponds to the $pn \to pn\eta$ reaction. In the experimental spectrum in addition to neutrons the peak from gamma rays is seen at a value of about 25 ns.

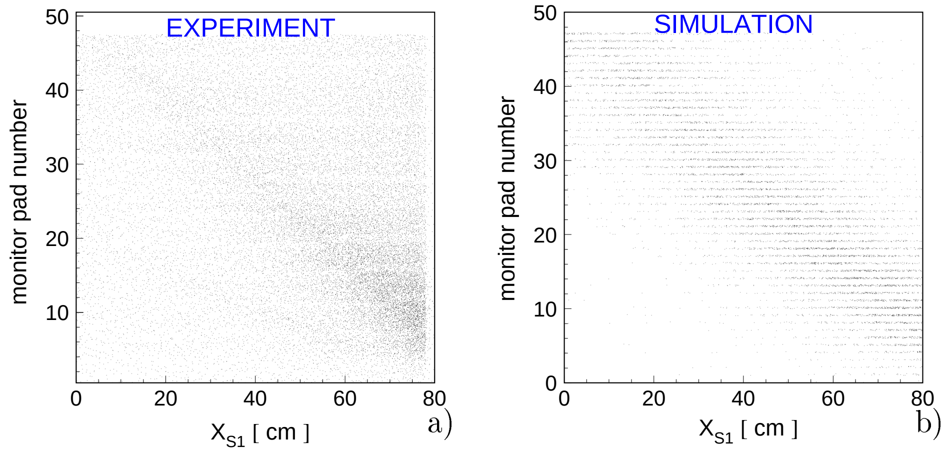

Figure 19: Luminosity evaluation via the quasi-free proton-proton scattering. Comparison between the simulation results and experimental data. Hit distribution from the experiment is not as uniform as the one from Monte-Carlo, since there is a strong dependence of the cross section on the scattering angle. Figures show the hit position in the Si_{mon} detector as a function of the hit position in the scintillator array S1 (see figure 11).

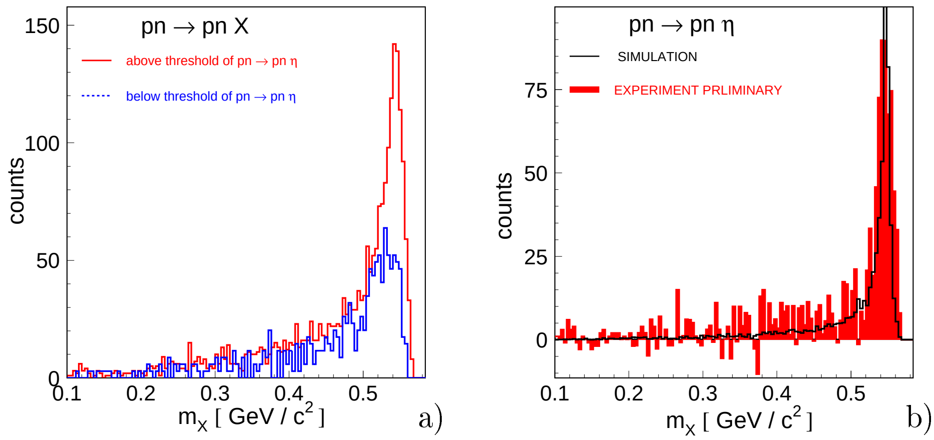

Figure 20: Missing mass spectra as obtained during the June'02 run:
a) Event distribution for $Q < 0$ (black line) and for $Q > 0$ (gray line).
b) Histogram represents the difference between number of events above and below threshold for the $pn \to pn\eta$ reaction, and the line corresponds to the Monte-Carlo simulation.

5 Estimation of the requested beam-time

Assuming a luminosity of $4{\cdot}10^{30}$ cm^{-2}s^{-1} (as obtained during the run this year), and taking into account i) the detection efficiency which decreases with excess energy as shown in Figure 13a and ii) the energy dependence of the total cross section as determined for the $pp \to pp\eta'$ reaction, we calculate the number of quasi-free $pn \to pn\eta'$ events which will be measured per day. The calculation can be performed modulo the absolute cross section which in the one extreme scenario should be equal to the cross section of the $pp \to pp\eta'$ reaction, and in the other extreme case should be enhanced by factor of about 6.5, as discussed in the introduction. The estimation results in 40 and 260 measured and reconstructed events per day for the extreme scenarios. The energy dependence of the total cross section is predominantly determined by the nucleon-nucleon final state interaction [24, 80], which approximately has the same influence for η and η' production. Thus, the observation that the excitation function for the $pp \to pp\eta$ and $pn \to pn\eta$ reaction is approximately the same justifies our assumption of the cross section dependence for the estimation of the counting rate.

In order to observe a signal from the $pn \to pn\eta'$ reaction with the statistical significance as this shown in figure 3, we would need to register about 5000 events. In figure 3 there are about 1500 events corresponding to the $pp \to pp\eta'$ reaction, however, the expected mass resolution for the $pn \to pn\eta'$ will be by factor of 3.5 worse. Thus, in the most optimistic case (260 events / day) we would require three weeks of beam time and in the most pessimistic one (40 events / day) 17 weeks. Our choice of 8 weeks is just the rough estimate of the average.

References

[1] K. Maltman, N. Isgur, Phys. Rev. **D 29** (1984) 952

[2] F. Kleefeld, M. Dillig, F. Pilotto, Acta Phys. Pol **B 27** (1996) 2867.

[3] S. Capstick et al., Presented at APS Division of Nuclear Physics Town Meeting on Electromagnetic and Hadronic Physics, Newport News, Virginia, 1-4 Dec 2000. e-Print Archive: hep-ph/0012238.

[4] S.D. Bass, S. Wetzel, W.Weise, Nucl. Phys. **A 686** (2001) 429.

[5] N. Nikolaev, CosyNews **No. 3** May 1998, Published by the Forschungszentrum Jülich in Cooperation with CANU, the COSY User Organisation of the Universities.

[6] E. Kou, Phys. Rev. **D 63** (2001) 054027.

[7] G.R Kalbfleisch et al., Phys. Rev. Lett. **12** (1964) 527.

[8] M. Goldberg et al., Phys. Rev. Lett. **12** (1964) 546.

[9] F.J. Gilman, R. Kauffman, Phys. Rev. **D 36** (1987), 2761,
see also Errata: Phys. Rev. **D 37** (1988) 3348.

[10] A. Bramon, R. Escribano, M.D. Scadron, Eur. Phys. J. **C 7** (1999) 271.

[11] D.J. Griffiths, *Introduction to Elementary Particles*,
John Wiley & Sons, Inc. New York 1987

[12] J.L. Rosner, Phys. Rev. **D 27** (1983) 1101.

[13] M.R. Pennington, DTP-90/68,
Proceedings of the Oxford Conference, September 1990

[14] M. D. Scadron, *Advanced Quantum Theory*, Springer-Verlag Berlin Heidelberg, 1991

[15] B. Diekmann, Phys. Rep. **159** (1988) 99.

[16] J.F. Donoghue, H. Gomm, Phys. Lett. **121B** (1983) 49.

[17] F. Lenz, Nucl. Phys. **B 279** (1987) 119.

[18] H.J. Lipkin, Phys. Lett. **B 67** (1977) 65.

[19] M. R. Ahmady, E. Kou, e-Print Archive: hep-ph/9903335.

[20] F. Araki, M. Musakhanov, H. Toki, Phys. Rev. **D 59** (1999) 037501.

[21] B. Tseng, Phys. Lett. **B 446** (1999) 125.

[22] H. J. Lipkin, Phys. Lett. **B 494** (2000) 248.

[23] H.-Y. Cheng, B. Tseng, Chin. J. Phys. **39** (2001) 28.

[24] K. Nakayama, e-Print Archive: nucl-th/0108032.

[25] N.I. Kochelev, V. Vento and A.V. Vinnikov, Phys. Lett. **B 472** (2000) 247.

[26] M. Dillig, *e–Print Archive* hep–ph/0202067

[27] M. Dillig, *e–Print Archive:* nucl–th/0201050

[28] S. D. Bass, Phys. Lett. **B 463** (1999) 286.

[29] S.D. Bass, *e–Print Archive:* hep–ph/0006348 and Proceedings of the *8th Int. Workshop On Deep Inelastic Scattering And QCD (DIS 2000)*, April 25–30, 2000, Liverpool, England;
Eds. J.A. Gracey and T. Greenshaw (World Scientific, Singapore, 2001), p.206

[30] S.D. Bass, Eur. Phys. J **A 5** (1999) 17.

[31] S. D. Bass, e-Print Archive: hep-ph/0006348.

[32] A. Ali, A.Ya Parkhomenko, e-Print Archive: hep-ph/0012212.

[33] P. Ball, J.-M. Frère, M. Tytgat, Phys. Lett. **B 365** (1996) 367.

[34] T. Muta, M.-Z. Yang, e-Print Archive: hep-ph/9902275.

[35] E. Kawai, Phys. Lett. **B 124** (1983) 262.

[36] C.P. Jessop et al., Phys. Rev. **D 58** (1998) 052002.

[37] G. Brandenburg et al., Phys. Rev. Lett. **75** (1995) 3804.

[38] D. Du, Y. Yang, G. Zhu, Phys. Rev. **D 59** (1999) 014007.

[39] H. Calén et al., Phys. Lett. **B 366** (1996) 39.

[40] H. Calén et al., Phys. Rev. Lett. **79** (1997) 2642.

[41] A. M. Bergdolt et al., Phys. Rev. **D 48** (1993) R2969.

[42] E. Chiavassa et al., Phys. Lett. **B 322** (1994) 270.

[43] F. Hibou et al., Phys. Lett. **B 438** (1998) 41.

[44] J. Smyrski et al., Phys. Lett. **B 474** (2000) 182.

[45] C. Wilkin, e-Print Archive: nucl-th/9810047.

[46] J. Haidenbauer, Ch. Hanhart, J. Speth, Acta Phys. Pol. **B 27** (1996) 2893.

[47] C. J. Horowitz, H. O. Meyer, D. K. Griegel, Phys. Rev. **C 49** (1994) 1337.

[48] Q. Zhao, e-Print Archive: nucl-th/0011070.

[49] B. Borasoy, Eur. Phys. J. **A 9** (2000) 95.

[50] G. 't Hooft, Phys. Rev. Lett. **37** (1976) 8.

[51] D. Lehmann, Eur. Phys. J. **A 4** (1999) 327.

[52] M. R. Ahmady, V. Elias, E. Kou, Phys. Rev. **D 57** (1998) 7034.

[53] P. Moskal et al., AIP Conf. Proc. **512** (2000) 65.

[54] V. Baru et al., Eur. Phys. J. **A 6** (1999) 445.

[55] E. Hernández, E. Oset, Phys. Lett. **B 350** (1995) 158.

[56] G. Fäldt, C. Wilkin, Z. Phys. **A 357** (1997) 241.

[57] J.-F. Germond, C. Wilkin, Nucl. Phys. **A 518** (1990) 308.

[58] J.M. Laget, F. Wellers, J. F. Lecolley, Phys. Lett. **B 257** (1991) 254.

[59] A. Moalem et al., Nucl. Phys. **A 600** (1996) 445.

[60] S. D. Bass, private communication

[61] K. Nakayama et al., Phys. Rev. **C 61** (2000) 024001.

[62] E. Gedalin, A. Moalem, L. Razdolskaja, Nucl. Phys. **A 650** (1999) 471.

[63] A. Sibirtsev and W. Cassing, Eur. Phys. J. **A 2** (1998) 333.

[64] R. Plötzke et al., Phys. Lett. **B 444** (1998) 555.

[65] F. Duncan et al., Phys. Rev. Lett. **80** (1998) 4390.

[66] H. Hahn et al., Phys. Rev. Lett. **82** (1999) 2258.

[67] F. Balestra et al., Phys. Lett. **B 491** (2000) 29.

[68] P. Moskal et al., Phys. Lett. **B 474** (2000) 416.

[69] P. Moskal et al., Phys. Rev. Lett. **80** (1998) 3202.

[70] P. Moskal et al., Phys. Lett. **B 482** (2000) 356.

[71] R. Bilger et al., Nucl. Instr. & Meth. **A 457** (2001) 64.

[72] H. Calén et al., Phys. Rev. **C 58** (1998) 2667.

[73] E. Chiavassa et al., Phys. Lett. **B 337** (1994) 192.

[74] M. Lacombe et al., Phys. Lett. **101B** (1981) 139.

[75] S. Häggström, Ph.D. thesis,
Uppsala University, Acta Universitatis Upsaliensis 13 (1997)

[76] M. Lacombe et al., Phys. Rev. **C21** (1980) 861.

[77] S. Brauksiepe et al., Nucl. Instr. & Meth. **A 376** (1996) 397.

[78] P. Moskal et al., Nucl. Instr. & Meth. **A 466** (2001) 448

[79] H. Dombrowski et al., Nucl. Instr. & Meth. **A 386** (1997) 228.

[80] F. Kleefeld, e-Print Archive: nucl-th/0108064.